IPMSM Inductances Calculation Using FEA

Dejan G. Jerkan, Marko A. Gecić and Darko P. Marčetić

Department for Power, Electronic and Telecommunication Engineering

Faculty of Technical Sciences, University of Novi Sad

Novi Sad, Serbia

dejan.jerkan@uns.ac.rs

Abstract – **Accurate determination of interior permanent magnet synchronous machine's (IPMSM) inductances is very important issue, especially in areas of high-performance drives and systems. This paper presents the method for calculation of the direct and quadrature inductances of permanent magnet synchronous machine using finite element analysis (FEA), where the calculation of these parameters is based on the determination of flux linkages. Two types of IPMSMs are investigated, with tangentially and radially magnetized permanent magnets. The results of the calculated inductances are presented by diagrams and they are discussed and compared with those obtained by measurements.**

Keywords – *Finite element analysis, direct and quadrature axis inductances, magnetic flux density, interior permanent magnet synchronous machine*

NOMENCLATURE

v_d, v_q – stator d- and q- axis voltages

i_d, i_q – stator d- and q- axis currents

$i_{a,b,c}$ – stator phase currents

R_s – stator phase resistance

Ψ_m – permanent magnet flux

L_d, L_q – stator d- and q- axis self inductances

Ψ_{ds} – stator d-axis flux

Ψ_{qs} – stator q-axis flux

ω – actual rotor angular speed

m_{el} – electromagnetic torque

m_m – load torque

J – motor inertia

p – number of pole pairs

ρ – saliency ratio (L_q/L_d)

J_s – current density vector

A_z – z component of the magnetic vector potential

μ – permeability of material

I.   INTRODUCTION

The interior permanent magnet synchronous motors (IPMSM) have many advantages, such as high power density and possibility for speed regulation in wide range of speeds [1], [7], [9]. IPMSMs are widely used in high-performance drives such as industrial robots and high-performance machine tools because of their advantages on high-torque with additional reluctant component. In recent years, the magnetic and thermal capabilities of the PM have been enhanced by employing permanent magnets with high coercitivity [1]. IPMSMs are used in more and more applications because of their small volume, very good efficiency, lower moment of inertia, rotor without heat problem, etc. [2]. Because of demands of high-performance drives it is very important to calculate as accurate as possible the values of the parameters of the IPMSM. Of the most important significance are the direct- and the quadrature- axis inductances, as they are determining corresponding synchronous reactances [3]. Also, they are the most important parameters when steady state and dynamic models of IPMSM are developed [4]. Unlike surface PM motors, which have the same value of inductance in direct and quadrature axes and where all the torque is produced by the magnet flux, interior permanent magnet motors have different direct and quadrature inductances which results in an additional torque component called reluctance torque [5]. The conventional methods of testing for determination of synchronous machine parameters are often inappropriate in the case of permanent magnet machines, because magnetic field produced by the permanent magnets cannot be canceled during measurements, and its field affects the total level of saturation of iron during experiments. On the other hand, finite element method provides great opportunities for accurate numerical analysis of IPMSM, because using FEA algorithms allows calculations of fundamental field quantities (such as flux linkages and stored magnetic energy), and also the fields produced by PMs can be canceled easily [6]. Standard experiments are reconstructing parameters of the machine based on quantities which can be measured through electrical connection of the machine, without knowledge of field distribution inside of the machine. During the last two decades the finite element method proved to be the most appropriate numerical method in terms of modeling, flexibility and accuracy to solve the nonlinear Poisson's equation governing the magnetic field who's concerned a principal element in calculation of machine parameters [6].

II. Equivalent circuit and basic equations

Fig. 1 shows the *d*- and *q*-axis equivalent circuits of IPMSM in which magnetic losses due to variable magnetic field in stator core are neglected. Based on Fig. 1 the mathematical equations of the equivalent *dq* axis steady state model of IPMSM in the rotor reference frame are given with:

$$\begin{bmatrix} v_d \\ v_q \end{bmatrix} = R_s \begin{bmatrix} i_d \\ i_q \end{bmatrix} + \begin{bmatrix} 0 & -\omega L_q \\ \omega L_d & 0 \end{bmatrix} \begin{bmatrix} i_d \\ i_q \end{bmatrix} + \begin{bmatrix} 0 \\ \omega \psi_m \end{bmatrix} \tag{1}$$

The electromagnetic torque of the IPMSM has two components: fundamental magnetic torque (which is proportional to the product of the magnet flux and *q*-axis stator current), and the reluctance torque (which is dependent on the saliency ratio and to the product of *dq*-axis stator current components). It is essential to determine IPMSM inductances to predict reluctance torque as an additional torque component. Based on Fig.1 torque can be expressed as:

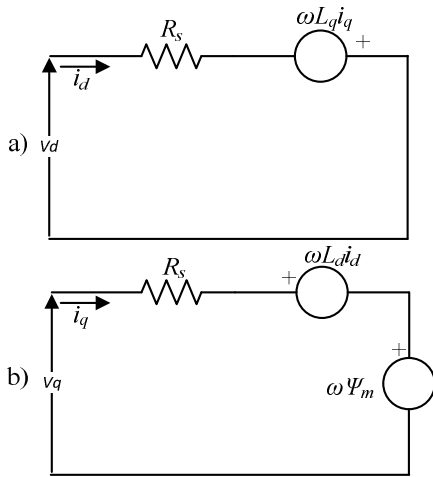$$T = \frac{3}{2} p \left(\Psi_m i_q + (1-\rho) L_d i_d i_q \right) \tag{2}$$

Figure 1. d- and q-axis equivalent circuits of IPMSM a) d-axis equivalent circuit, b) q-axis equivalent circuit

III. Finite Element Analysis of IPMSM

The finite element analysis is used in many areas of technical sciences, such as magnetics, electrostatic problems, heat transfer, fluid dynamics etc. All FEA algorithms are based on solution of field equations over domain of interest using division of that domain with small segments of simple geometric shapes, called finite elements (in 2-D FEA the most common are triangular shapes), in order to reconstruct the field of the entire domain. Values of field variables inside any of the elements are represented using 2-D interpolation functions [6]. These functions are defined on each element using the values of the calculated variable in each node.

Knowing the value of variable of interest in every node of the region, combined with the usage of interpolation functions allows complete definition of the behavior of the variable field on each element. The precision of the method depends not only on the dimensions of elements and their number but also on the type of the interpolation function. As for the numerical method, the FEA algorithm converges to the exact solution provided to increase the number of subdivisions of the solution domain and to ensure continuity of the interpolation function of its first derivatives along the borders of adjacent elements [6]. FEA algorithms used in the problems of electrical machines analysis are based on the evaluation of the magnetic vector potential A. As already mentioned, 2-D FEA algorithm will be used in this research, and the starting equation for FEA is given by:

$$-\frac{\delta}{\delta x}\left(\frac{1}{\mu}\left(\frac{\delta A_z}{\delta x}\right)\right) - \frac{\delta}{\delta y}\left(\frac{1}{\mu}\left(\frac{\delta A_z}{\delta y}\right)\right) = J_s \tag{3}$$

Equation (3) is used for magneto-static solutions, so there is no time varying of currents or motion of rotor.

Adequate usage of FEA algorithms demands definition of proper boundary conditions, which determine how lines of magnetic potential vector pass through areas that separate regions with different magnetic properties. Analyzed machines have small area of 2-D cross-section (please see Table 1 for machine's dimensions), so only one boundary condition needs to be defined for this type of FEA, so-called *Dirichlet* boundary condition, and the most common use of it is to define $A_z=0$ along outer stator surface. This means that with this boundary condition we force the magnetic field to stay inside boundary defined by stator outer diameter. For larger geometries it is useful to define additional boundary conditions which allow usage of only one slice of machine's geometry, and the width of that slice is defined by pole width, which means that for large machines with large number of pole pairs these boundary conditions can speed-up the simulations considerably [6].

FEA algorithm solves equation (3) for every node of the mesh created by division of region of interest with finite elements using some of well-known numerical algorithms, such as Newton-Raphson's, for instance. After finding values of A_z in all nodes of meshed region, calculating flux linkages of specific phase windings can be done easily. The flux linkage Ψ_{ij} of the j-th winding when the i-th winding is supplied with current can be expressed by [7]:

$$\Psi_{ij} = p\frac{1}{S_j}\left(\int_{\Omega_j^+} A_z d\Omega - \int_{\Omega_j^-} A_z dS\right) N_j l_j \tag{4}$$

where N_j is the number of turns of j-th winding, l_j is the length of the stator core and S_j is the cross-section of the coil

region. Ω_j^+ and Ω_j^- represent the positive and negative trace of the winding in (x,y) plane. The flux vector in d-q domain can be formed as follows:

$$\Psi = \Psi_{ds} + j\Psi_{qs} = \frac{2}{3}(\Psi_a + a\Psi_b + a^2\Psi_c) \tag{5}$$

$$\Psi_{ds} = \frac{2}{3}(\Psi_a - \frac{1}{2}\Psi_b - \frac{1}{2}\Psi_c) \tag{6}$$

$$\Psi_{qs} = \frac{1}{\sqrt{3}}(\Psi_b - \Psi_c) \tag{7}$$

IV. INDUCTANCE CALCULATION

Accurate inductance calculation of PMSM is a relevant topic, since the inductances determine large part of the electrical machine behavior [1]. The inductances estimation in the d-q axis is crucial not only for determination of the torque and flux weakening capability but also for designing control systems in order to optimize the efficiency, power factor, etc. [3]. In this paper two types of IPMSM geometries will be analyzed. Both types have identical stator (three-phase four-pole concentrated winding), and the rotors are chosen in such a way to represent two most significant types of PM orientation used in IPMSMs. First type, here called IPMSM-T (Figure 2a) is with tangentially magnetized PMs, and the second one, here called IPMSM-R (Figure 2b) is with radially magnetized PMs. Figure 3 and 4 respectively show PMs air-gap flux distribution for the two mentioned types of motors. It is well known that in the type IPMSM-R quadrature inductance Lq is greater than direct inductance Ld, because there is more iron along q axis (Figure 2b). However, such conclusion is not so straightforward for the type IPMSM-T, because PMs flux path is between two neighboring magnets, which means through iron (which increases the inductance), but the flux path is much longer (which decreases the inductances).

The first FEA simulation will be used to calculate Ld. The magnet flux is turned off by setting the magnet remanence Br to zero. The current vector must be aligned with the d axis. Variation of inductance as a function of current amplitude is of interest, so series of magneto-static simulations with different levels of current excitation will be conducted in order to obtain these relationships. For example, if the magnitude of stator current is chosen to be 1A, then to align the current axis with phase a axis the instantaneous phase currents have to be defined as:

$$i_a = 1A \ , \ i_b = i_c = -\frac{i_a}{2} = 0.5A \tag{8}$$

The d and q components of the current vector are then defined as:

$$i_d = 1A \ , \ i_q = 0A \tag{9}$$

Figures 5 and 7 respectively show the field solution for this case, for both types of IPMSM. The flux linkages of phases a, b and c are then calculated using equation (4). The flux vector is constructed and it's direct and quadrature components are calculated using expressions (6) and (7). It is important to state

that the 2-D FEA simulation neglects the leakage flux in the end region, because it cannot be included without usage of 3-D FEA algorithm [8], [9]. Analyzed machines have concentrated winding, which means that they have very short end connections, especially in comparison with distributed windings. Because of that, one may expect very small end turn leakage inductances. However, their influence can be included by adding some analytical expressions [7] on calculated inductances, or by comparing the 2-D FEA results with measurements, because measured inductances include those effects. In this paper end connections leakage inductances have been neglected.

The inductances Lq are calculated in a similar manner, only this time the current vector needs to be aligned with the q axis. The phase currents are then given as:

$$i_a = 0A \ , \ i_b = -i_c = \frac{\sqrt{3}}{2}A \tag{10}$$

The d and q components of the current vector are then defined as:

$$i_d = 0A \ , \ i_q = 1A \tag{11}$$

Figures 6 and 8 show the field solution for this case, for both types of IPMSM. After calculating the flux components, the inductances for one turn per coil are given by:

$$L_d = \frac{\Psi_{ds}}{i_d} \ , \ L_q = \frac{\Psi_{qs}}{i_q} \tag{12}$$
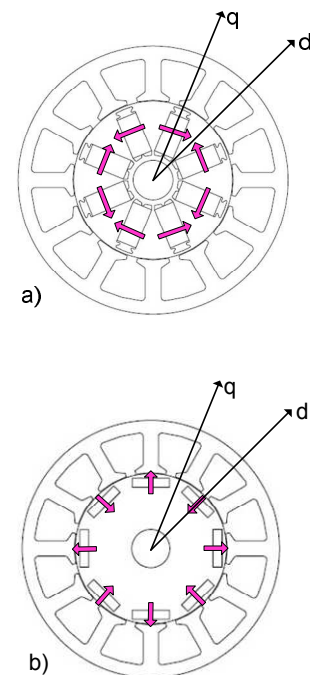
Figure 2. Two types of IPMSM: a) IPMSM with tangentially magnetized PMs (IPMSM-T), b) IPMSM with radially magnetized PMs (IPMSM-R)
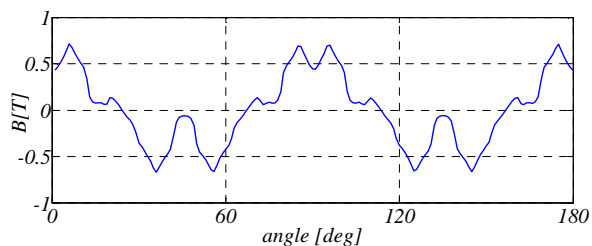
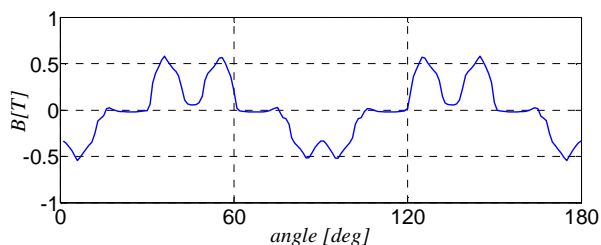Figure 3. Flux distribution of permanent magnets in air gap of IPMSM-T

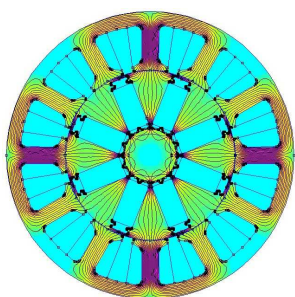Figure 4. Flux distribution of permanent magnets in air gap of IPMSM-R

Figure 5. Distribution of flux lines in IPMSM-T when there is only d axis current in stator windings
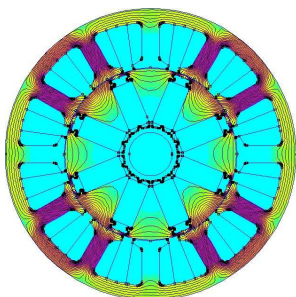

Figure 6. Distribution of flux lines in IPMSM-T when there is only q axis current in stator windings
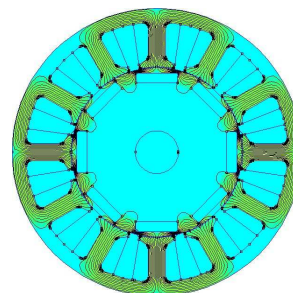

Figure 7. Distribution of flux lines in IPMSM-R when there is only d axis current in stator windings
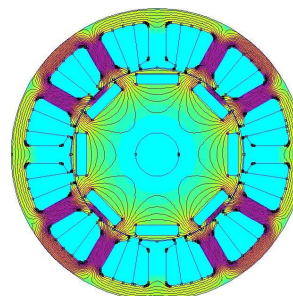

Figure 8. Distribution of flux lines in IPMSM-R when there is only q axis current in stator windings

V. RESULTS OF INDUCTANCE CALCULATIONS

Rated parameters for IPMSM-T machine are given in Table 1, and IPMSM-R machine was generated for the sake of comparison with IPMSM-T configuration. As mentioned above, both machines have the same stator. Results of calculations described in previous chapter are shown in Figures 9 (for inductance Ld) and 10 (for inductance Lq). It is interesting to notice that for both types of IPMSMs quadrature inductance Lq is approximately 50% greater than direct inductance Ld, and that inductance Ld is more influenced by saturation. Results are showing good match with experimental results (existent only for type IPMSM-T), but there are some difference between simulations and experiments (both Ld and Lq calculated with FEA are approx. 10% larger from those obtained with experiments). This can be explained by the fact that PMs cannot be excluded from experiments without destroying the rotor, and their field is added on time-varying field produced by excitation during experiments, which has influence on saturation level during measurement. Also, for the purpose of FEA simulations authors did not have precise data for steel used for stator stack (relative permeability as a function of field strength).
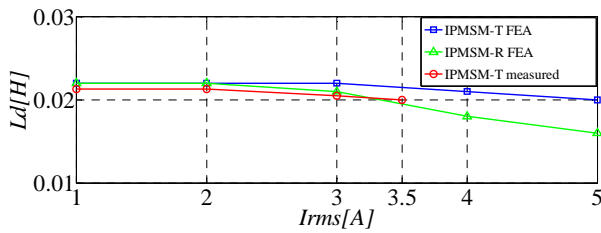
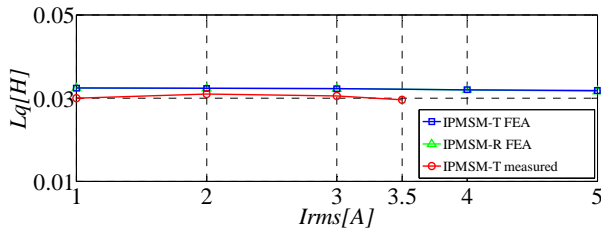Figure 9.   Results of FEA simulations and measurements for direct axis inductance Ld

Figure 10. Results of FEA simulations and measurments for quadrature axis inductance Lq

TABLE I.   IPMSM-T NAMEPLATE DATA

IPMSM-T rated data	Values
Number of stator slots	12
Number of poles	8
Stator core outside dimension [mm]	102
Stator core stack thikness [mm]	42
Stator core inside diameter [mm]	60.6
Air gap width [mm]	0.3
Winding specification	φ0.65×84T, Y ,Al
Resistance (2 phase) 20°C	7.5Ω
Direct and quadrature inductances [mH]	Ld=20.8 Lq=30.1
Rated speed [rpm]	500
Rated torque [Nm]	1.00

VI.   CONCLUSION

In this paper, the method for calculation of inductances for two types of IPMSMs was presented. The method is based on the FEA calculation of flux linkages. It was shown that the quadrature inductance Lq is greater than direct inductance Ld for both types of motors. Further research using FEA software combined with measurements may be useful for determination of end connection leakage inductance influence, and also to investigate saturation of q axis flux path because of the presence of permanent magnets. Results for type IPMSM-T are showing good match with the results from the manufacturer of the machine. Presented method can be useful for detail analysis of different constructions of IPMSM with possibility to separate influence of excitation from influence of permanent magnets field, which cannot be done easily during measurements.

VII.   REFERENCES

F. Shiferl, T.A. Lipo, "Power Capability of Salient Pole Permanent Magnet Synchronous Motors in Variable Speed Drive Applications", IEEE Trans. Ind. Appl., vol. 26, pp. 115–123, Jan./Feb. 1990.

Y. Li, X.P. Yan, "The perspective and status of PMSM electrical servo system," *Micromotors Servo Technique*, vol. 4, pp. 30-33, 2001.

M. Pastorelli, J. Bottomley, P. Giangrande and C. Gerada, "Sensorless control of PM motor drives — A technology status review," IEEE Work. Elec. Mach. Design Contr. Diag. (WEMDCD), vol. 48, no. 4, pp. 168–182, March 11-12, 2013.

K. Jang-Mok and S. Seung-Ki, "Speed control of interior permanent magnet synchronous motor drive for the flux weakening operation," IEEE Trans. Ind. Appl., vol. 33, no. 1, pp. 43–48, January/February 1997.

D. Zarko, "A Systematic Approach to Optimized Design of Permanent Magnet Motors With Reduced Torque Pulsations", Pd.D. thesis, University of Winsconsin-Madison, USA, 2004.

P. Silvester, "Finite Elements for Electrical Engineers", Cambridge University Press, 1990.

[7]   J. Cros and P. Viarouge, "Synthesis of High Performance PM Motors With Concentrated Windings", IEEE Trans. Energy. Conv., vol. 17, no. 2, pp. 248-253, Jun 2002.

[8]   T. Cox, F. Eastham, and J. Proverbs, "End Turn Leakage Reactance of Concentrated Modular Winding Stators," IEEE Transactions on Magnetics, vol. 44, no. 11, pp. 4057-4061, November 2008.

[9]   A. M. EL-Refaie, "Fractional - Slot Concentrated-Windings Synchronous Permanent Magnet Machines: Opportunities and Challenges", IEEE Trans.Ind. El., vol. 57, no. 1, January 2010.